

## Johnson Matthey Highlights

### A selection of recent publications by Johnson Matthey R&D staff and collaborators

#### Catalyst-Directed Chemoselective Double Amination of Bromo-chloro(hetero)arenes: A Synthetic Route toward Advanced Amino-Aniline Intermediates

A. A. Mikhailine, G. A. Grasa Mannino and T. J. Colacot, *Org. Lett.*, 2018, **20**, (8), 2301

Amino-anilines and their derivatives were prepared *via* a chemoselective sequential one-pot coupling protocol. The benefits of such a protocol include increases in safety, economics and process efficiency. Pd-allyl complexes were used as precatalysts for the amination of (hetero)aryl substrates with biologically active secondary amines and the type of catalyst used influenced nucleophile and site selectivity. For instance, the Pd-based RuPhos or (BINAP)Pd(allyl)Cl precatalyst selectively coupled the Ar-Cl site with secondary amines. The practical applications for this work include the preparation of amino-anilines as the building blocks for active pharmaceutical ingredients (APIs). This was demonstrated through the synthesis of a precursor used in the preparation of the oncology drug Brigatinib.

#### Development of Concise Two-Step Catalytic Approach Towards Lasofoxifene Precursor Nafoxidine

C. C. C. Johansson Seechurn, I. Gazić Smilović, T. Colacot, A. Zanotti-Gerosa and Z. Časar, *Bioorg. Med. Chem.*, 2018, **26**, (9), 2691

The shortest two-step catalytic approach to nafoxidine (a precursor to lasofoxifene) from the starting material tetralone is demonstrated with an overall yield of 55% and low Pd catalyst loading 0.1 mol%. The first step involved  $\alpha$ -arylation of 6-methoxy-3,4-dihydronaphthalen-1(2H)-one with chlorobenzene to provide 6-methoxy-2-phenyl-3,4-dihydronaphthalen-1(2H)-one in 90% yield. The second step was the conversion of 6-methoxy-2-phenyl-3,4-dihydronaphthalen-1(2H)-one to nafoxidine in 61% yield, which

occurred *via* a CeCl<sub>3</sub> promoted reaction with (4-(2-(pyrrolidin-1-yl)ethoxy)phenyl)lithium. This work offers a promising alternative to the primary synthetic three-step route to lasofoxifene, by reducing the amount of waste generated and the unit operations required. The two-step approach to nafoxidine is also more cost effective in comparison.

#### Using Neutrons, X-rays and Nuclear Magnetism to Determine the Role of Transition Metal Oxide Inclusions on both Glass Structure and Stability in Automotive Glass Enamels

D. T. Bowron, J. Booth, N. S. Barrow, P. Sutton and S. R. Johnson, *Phys. Chem. Chem. Phys.*, 2018, **20**, (20), 13734

Automotive glass enamels were doped with transition metal oxides. X-ray scattering, neutron scattering and solid-state nuclear magnetic resonance (NMR) techniques were used to investigate the effects this had on crystallisation and phase separation properties. The addition of iron oxide had considerable effects on the optical properties of the glass. The addition of 2.5% manganese oxide suppressed crystallisation of an undesirable bismuth silicate (Bi<sub>2</sub>SiO<sub>5</sub>) phase. This could be utilised to influence automotive glass enamel properties to meet product requirements. There is suggestion for further investigations to focus on manganese oxidation states as a function of doping level, and for the use of additional techniques such as Raman.

#### Catalytic Depolymerisation of Suberin Rich Biomass with Precious Metal Catalysts

C. S. McCallum, N. Strachan, S. C. Bennett, W. G. Forsythe, M. D. Garrett, C. Hardacre, K. Morgan and G. N. Shelldrake, *Green Chem.*, 2018, **20**, (12), 2702

A range of precious metal catalysts were used to investigate the hydrogenolysis of cork and particular attention was given to the impact of the

type of solvent, support and base. In comparison to the absence of a catalyst, the incorporation of a catalyst and a base resulted in increases in lipid yield of 113–258% and bio-oil increases of 9.3–158%. With the addition of a base, the bio-oil yield increased from 11.5 wt% to 42.6 wt% and allowed use of a 'greener' solvent. There were also increases in the conversion of solid materials (48.7 wt%).

#### The UN Sustainable Development Goals: How can Sustainable Chemistry Contribute? A View from the Chemical Industry

S. Axon and D. James, *Curr. Opin. Green Sustain. Chem.*, 2018, **13**, 140

The United Nations Sustainable Development Goals are discussed, with reference to examples from the chemical industry. Suggestions are made for key stakeholders in the chemical industry to increase their efforts and ensure effective delivery of the goals. This includes education and training providers, national and international funding bodies, industrial chemical companies, chemical societies and businesses. An evaluation of the tools companies use to aid the achievement of the goals is provided. It is suggested that sharing best practices across the chemical industry could lead to the development of a systematic tool to assess the manufacture and use of chemical products.

#### Morphological Transformations During Drying of Surfactant-Nanofluid Droplets

A. Osman, N. Shahidzadeh, H. Stitt and N. Shokri, *J. Ind. Eng. Chem.*, 2018, **67**, 92

Surfactants were grouped according to alkyl chain length and the effect of each surfactant type on the drying dynamics of silica nanosized dispersion droplets was investigated. An acoustic levitator was used to perform single droplet drying experiments. The final morphology of the grains formed at the end of the drying process was characterised using SEM. Surfactant molecular weight had a significant influence on the morphology of the grains. For instance, more irregular grains were observed when drops with high molecular weight surfactants were dried. Hollow dried grains were observed as the result of surface tension instability.

#### Adhesive Strength Measurement of Catalyst Support

J. Yang, P. Blanco-García, E. M. Holt, A. Wagland, K. Huang and A. D. Salman, *Powder Technol.*, 2018, **340**, 465

A novel technique was developed to measure the adhesive strength of a coated catalyst layer. To produce the coated layers, a  $\gamma$ -alumina suspension of known particle size distribution and pH was dried on three different substrates (FeCrAlloy, cordierite

and alumina). The porosity, pH and surface roughness of the substrate had an impact on adhesive strength. For the cordierite and FeCrAlloy substrates the adhesive strength peaked at pH = 4. At higher pH levels, the coated layer detached from the substrate after drying. The surface roughness of the cordierite substrate led to increased adhesive strength. Alumina substrates had reduced porosity and higher adhesive strength.

#### Impact of Bio-Alcohol Fuels Combustion on Particulate Matter Morphology from Efficient Gasoline Direct Injection Engines

C. Hergueta, A. Tsolakis, J. M. Herreros, M. Bogarra, E. Price, K. Simmance, A. P. E. York and D. Thompsett, *Appl. Energy*, 2018, **230**, 794

TEM was used to perform morphological analysis of particulate emissions from the combustion of two bio-alcohol blends (25% v/v ethanol in gasoline, 33% v/v butanol in gasoline) and commercial gasoline. It was observed that the primary particles emitted from the combustion of ethanol-gasoline and butanol-gasoline blends were smaller than those released from gasoline. Combustion of the butanol-gasoline blend significantly increased particle oxidation, with an 80% reduction in particle concentration in the engine exhaust in comparison to gasoline. The ethanol-gasoline blend demonstrated more chain-like particles, making particles emitted from this type of combustion easier to trap than those from gasoline combustion.

#### Liquid-Phase Parametrization and Solidification in Many-Body Dissipative Particle Dynamics

P. Vanya, P. Crout, J. Sharman and J. A. Elliott, *Phys. Rev. E*, 2018, **98**, (3), 033310

Many-body dissipative particle dynamics (MDPD) was studied after a gap in the exploration of this mesoscale method was identified. The properties and structure of an MDPD fluid were systematically investigated. It is known that MDPD can, in a single simulation, reproduce liquid-vapour coexistence. This study demonstrated the dependence of surface tension and density on the interactive parameters in this liquid phase. The authors developed a top-down parametrisation for real liquids. This study also revealed that MDPD can yield a thermodynamically stable solid phase and a gas phase.

#### Effect of Pretreatment Method on the Nanostructure and Performance of Supported Co Catalysts in Fischer-Tropsch Synthesis

R. W. Mitchell, D. C. Lloyd, L. G. A. van de Water, P. R. Ellis, K. A. Metcalfe, C. Sibbald, L. H. Davies, D. I. Enache, G. J. Kelly, E. D. Boyes and P. L. Gai, *ACS Catal.*, 2018, **8**, (9), 8816

Dried reduced (D) and dried calcined reduced (DC) Co catalysts were synthesised on various reducible

and nonreducible supports commonly used in Fischer-Tropsch applications ( $\text{SiO}_2$ ,  $\text{Al}_2\text{O}_3$ ,  $\text{TiO}_2$ , and  $\text{ZrO}_2$ ). The formation of active catalyst phases in the supported Co catalysts was systematically analysed using *in situ* environmental (scanning) transmission electron microscopy (E(S)TEM) and several other techniques. The D samples showed higher activity rates than the DC catalysts, regardless of the support used and this can be partially attributed to better dispersion of Co active species (**Figure 1**). Observations showed that nonreducible supports promoted more highly dispersed small Co metal species and therefore more active sites.

#### An EPR Investigation of Binding Environments by N-Donor Chelating Exchange Resins for Cu Extraction from Aqueous Media

J. Spencer, J. Stevens, C. Perry and D. M. Murphy, *Inorg. Chem.*, 2018, **57**, (17), 10857

Dowex™ M4195 and CuWRAM are chelating exchange resins used for Cu(II) extraction in aqueous media. Electron paramagnetic resonance (EPR) spectroscopy and UV-vis spectroscopy were employed to characterise Cu(II) binding environments within these resins. Two dominant intramolecular species were characterised for each resin:  $[\text{Cu}^{\text{II}}(\text{BPA})](\text{H}_2\text{O})_m$  and  $[\text{Cu}^{\text{II}}(\text{BPA})_2]$  for Dowex™ M4195 and  $[\text{Cu}^{\text{II}}(\text{PA})_2](\text{H}_2\text{O})_m$  and  $[\text{Cu}^{\text{II}}(\text{PA})_3]$  for CuWRAM.  $[\text{Cu}^{\text{II}}(\text{BPA})_x(\text{BPA})_y(\text{H}_2\text{O})_n]$  and  $[\text{Cu}^{\text{II}}(\text{PA})_x(\text{PA})_y(\text{H}_2\text{O})_n]$  were two additional intermolecular species identified on both resins. Dehydration-rehydration and acid elution studies were performed. Experiments demonstrated that the intermolecular species were less strongly coordinated to the resins in comparison with the intramolecular species. The Dowex™ M4195 material had a higher Cu(II) capacity in comparison to CuWRAM.

#### Towards High Performance Metal–Organic Framework–Microporous Polymer Mixed Matrix Membranes: Addressing Compatibility and Limiting Aging by Polymer Doping

A. Sabetghadam, X. Liu, A. F. Orsi, M. M. Lozinska, T. Johnson, K. M. B. Jansen, P. A. Wright, M. Carta, N. B. McKeown, F. Kapteijn and J. Gascon, *Chem. Eur. J.*, 2018, **24**, (49), 12796

The development of mixed matrix membranes (MMMs) for use in membrane separation for gas

purification has been a challenge due to the absence of a simple method for reflecting the properties of the components (e.g. fillers and polymers) in the final membrane performance. The authors describe the development of MOF-based MMMs which demonstrate superior separation properties and low aging rates. This was achieved by combining small amounts of a glassy polymer with high performance PIM-1. The commercial target for post-combustion  $\text{CO}_2$  capture was met.

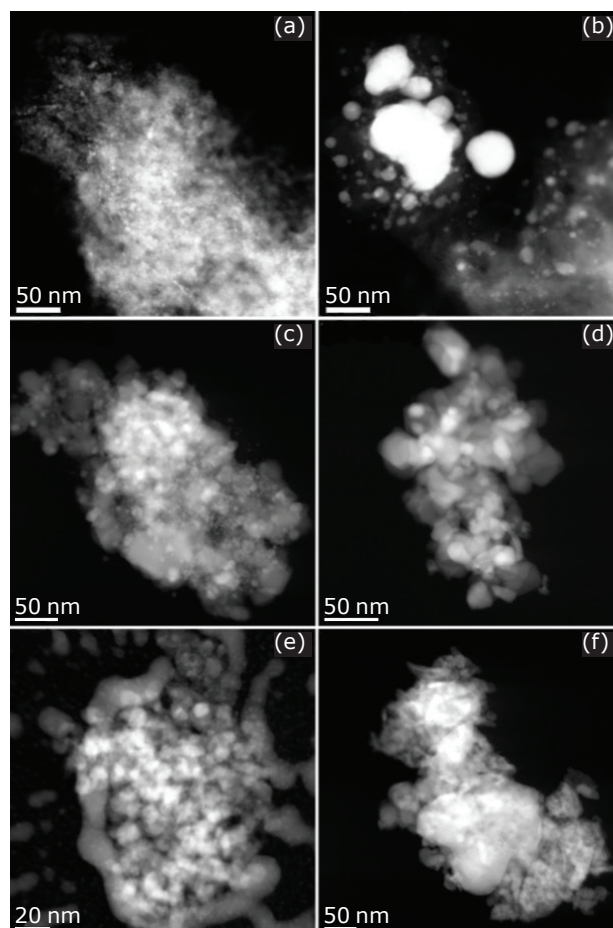


Fig. 1. STEM-HAADF images illustrating the distribution of Co particles following  $\text{H}_2$  reduction at  $400^\circ\text{C}$  in: (a) dried reduced  $\text{Co}/\text{Al}_2\text{O}_3$ ; (b) dried calcined reduced  $\text{Co}/\text{Al}_2\text{O}_3$ ; (c) dried reduced  $\text{Co}/\text{TiO}_2$ ; (d) dried calcined reduced  $\text{Co}/\text{TiO}_2$ ; (e) dried reduced  $\text{Co}/\text{ZrO}_2$ ; (f) dried calcined reduced  $\text{Co}/\text{ZrO}_2$ . Reprinted with permission from R. W. Mitchell *et al.*, *ACS Catal.*, 2018, **8**, (9), 8816. Copyright 2018 American Chemical Society